Journal of Power Sources 185 (2008) 1492–1498

Contents lists available at ScienceDirect

Journal of Power Sources

journal homepage: www.elsevier.com/locate/jpowsour

# Improved stability of quasi-solid-state dye-sensitized solar cell based on poly (ethylene oxide)–poly (vinylidene fluoride) polymer-blend electrolytes

Ying Yang[a], Cong-hua Zhou[a], Sheng Xu[a], Hao Hu[a], Bo-lei Chen[a], Jing Zhang[a], Su-juan Wu[a], Wei Liu[a], Xing-zhong Zhao[a,b,*]

[a] Department of Physics, Wuhan University, Wuhan 430072, People's Republic of China
[b] Key Laboratory of Acoustic and Photonic Materials and Devices of Ministry of Education, Wuhan University, Wuhan 430072, People's Republic of China

ARTICLE INFO

*Article history:*
Received 16 May 2008
Received in revised form
11 September 2008
Accepted 11 September 2008
Available online 19 September 2008

*Keywords:*
Hydroxyl-rich small-molecule additives
Water
Ethanol
Cross-linking network

ABSTRACT

We report two improved stability dye-sensitized $TiO_2$ solar cells using poly (ethylene oxide)–poly (vinylidene fluoride) (PEO–PVDF) polymer-blend electrolytes modified with water and ethanol as hydroxyl-rich small-molecule additives. The effect of additive on the thermal property, viscosity, conductivity and the corresponding performance of the dye-sensitized solar cell (DSSC) were studied. After introducing the water and ethanol into the PEO–PVDF polymer-blend electrolytes, the conductivity is improved compared to that of the un-added electrolyte. This is due to the enhanced free ion concentration and ion transport channels in the electrolyte because of the cross-linking ability of these hydroxyl-rich additives. The increased ion concentration can be proved by the enhanced concentration of $I^-$ and $I_3^-$ in the additive-modified electrolytes from UV–vis studies. The increased cross-linking network can be explained by the increased glass transition temperature ($T_g$) and viscosity of these additive-modified electrolytes from DSC and rheology studies. A more homogeneous morphology of ethanol-modified electrolyte from SEM study is used to further explain the better conductivity and stability of the cells based on these additive-modified electrolytes. From the evaluation of additive effect on the performance of the corresponding DSSC, we find that introducing water and ethanol leads to an increase in short-circuit photocurrent density ($J_{sc}$). This is due to the efficient transport of $I^-/I^{3-}$ caused by enhanced $I^-/I^{3-}$ concentration and increased ion transport channels in the electrolyte by adding additives. The best efficiency of 3.9% is achieved in the cell with ethanol-modified electrolyte.



## 1. Introduction

Dye-sensitized solar cell (DSSC) has been attracting much attention as a more efficient, clean and low cost energy storage method, which was first reported by Grätzel [1]. Although a photo-to-current conversion efficiency of more than 11% has been achieved in a liquid electrolyte-based DSSC [2], the major drawback of these solar cells is the poor long-term stability owing to the evaporation of the liquid phase in the cells. To improve the stability of DSSC, many efforts have been made to replace the liquid electrolyte by solid-state medium, such as, inorganic p-type semiconductors [3], organic hole-transport materials [4], room-temperature molten salts [5–7], polymer–gel electrolytes [8,9], and solid polymer redox electrolytes [10,11]. Among these studies, quasi-solid-state polymer electrolyte might be a better choice to increase ionic conductivity and stability because there is a small amount of solvent remaining but no solvent leakage in this type of electrolyte.

Recently, Xia et al. [12] reported on the stability performance of a quasi-solid-state DSSC employing a liquid electrolyte added with poly (propylene oxide) (PPO), poly (ethylene oxide) (PEO) or poly (ethylene oxide)-block-poly (propylene oxide)-block-poly (ethylene oxide) ($P_{123}$). In this study, an improved stability was observed in these polyether added electrolyte, which originated from the existence of a number of channels between the anode and cathode to maintain the liquid electrolyte from evaporation and consequently improved the stability of DSSC. Kubo et al. [13] reported a highly stable DSSC (stable at 5% for almost 1000 h) using a gelated 1-alkyl-3-methylimidazolium iodide-based ionic liquid electrolyte.

In a quasi-solid-state polymer electrolyte, framework materials play an important role in maintaining the stability of DSSC by offering a liquid-like channel for the triiodide ($I_3^-$)/iodide ($I^-$) diffusion. Some gelators have been used as framework materials to modify the polymer electrolyte in DSSC [14–16]. A gelator is expected to induce important intrinsic modifications in local structure; release

* Corresponding author at: Department of Physics, Wuhan University, Wuhan 430072, People's Republic of China. Tel.: +86 27 87642784; fax: +86 27 68752569.
*E-mail address:* xzzhao@whu.edu.cn (X.-z. Zhao).

0378-7753/$ – see front matter © 2008 Elsevier B.V. All rights reserved.
doi:10.1016/j.jpowsour.2008.09.034

mobile charge carriers due to ion dissolution effect and introduce a new path for ion transport through cross-linking effect of gelators [17]. The overall effect leads to an increase in the number of mobile charge carriers and results in an ionic transport behavior resembling that of a liquid system [18]. The chain length of the gelators should be as low as possible to realize sufficient ion mobility and to avoid the crystallization of the gelator within the gel electrolyte [19]. So, small-molecule gelator is the choice for improving the electrochemical properties of the polymer electrolyte.

Polymer blending technique is extensively used in preparing polymer electrolyte to get better electrical properties. Jacob et al. [19] reported a solid polymer electrolyte by introducing poly (vinylidene fluoride) (PVDF) into a PEO–$LiClO_4$ system, which increased the ionic conductivity by two orders of magnitude. And PVDF, with the presence of fluorine which has the smallest ionic radius and the largest electronegativity, is expected to improve the ionic transport and reduce the recombination rate at semiconductor/polymer electrolyte interface in DSSC. Since 2004, a series of polymer electrolytes based on poly (ethylene oxide)–poly (vinylidene fluoride) (PEO–PVDF) polymer blend have been studied in our group [20,21]. The compatibility and photoelectrochemical behavior of polymer-blend electrolyte by introducing PVDF and $TiO_2$ into PEO have been studied [21]. This solid electrolyte based on PEO–PVDF showed good miscibility and improved ionic conductivity and achieved a high photo-to-current conversion efficiency of 4.8% under the illumination of 65.2 mW $cm^{-2}$ (AM 1.5), comparing to that of pure PEO polymer electrolyte.

As it is known, the stability of DSSC is a crucial issue considering its practical application. However, there is few literature concerning on the stability of DSSC based on polymer electrolytes. In this paper, we attempt to study the effect of hydroxyl-rich small-molecule additives (water and ethanol) on the stability of cells with PEO–PVDF/$TiO_2$ polymer electrolyte, expecting the addition of these additives to form cross-linking network among poly (ethylene oxide) (PEO), $TiO_2$ and lithium iodide (LiI) in the electrolyte and achieve better long-term stability of the cells. We also investigated the additive effect with respect to the thermal properties, viscosity properties, surface morphology and ionic conductivity of the PEO–PVDF polymer-blend electrolyte.

## 2. Experimental

### 2.1. Reagent

Poly (ethylene oxide) ($M_w = 2\times10^6$ g $mol^{-1}$, Aldrich), Poly (vinylidene fluoride) ($M_w = 1\times10^5$ g $mol^{-1}$, Shanghai, China), Lithium iodide (99%, Acros), iodine ($I_2$, 99.8%, Tianjin, China), propylene carbonate (PC, 99.9%, anhydrous, SCRC, China), 1,2-dimethoxyethane (DME, 99.0%, SCRC, China), $TiO_2$ (P25, 20–30 nm, Degussa AG, Germany) deionized water and ethanol were used in this study. Solid-state chemicals were stored in vacuum desiccators before use and used without further purification.

### 2.2. Preparation of PEO–PVDF polymer-blend electrolytes

In our experiment, 0.4 g polymer blend with PEO/PVDF = 2:3 wt.% were dissolved into 15 g DME/PC (3:7, v/v) co-solvent, then 0.5 g (3.1 wt.%) water and ethanol were added, respectively, into the above mixed solution under continuous stirring at 80 °C in silicone bath. After about 4 h, $TiO_2$ (P25) nanoparticles (0.0582 g) were slowly introduced. This mixed solution was stirred at 80 °C for another 2 h. Then the solid LiI and $I_2$ with LiI concentration of 28.9 wt.% (EO:Li = 3) and LiI/$I_2$ = 10:1 (molar ratio) were added to the above polymer solution at ambient environment. (Here, the "LiI concentration" means LiI/(PEO + PVDF + LiI).) The polymer solution was stirred continuously for almost 4 days in the hermetic brown flask until a homogeneous viscous liquid was formed. The polymer-blend electrolyte membranes for FTIR measurements were prepared by casting the polymer-blend solutions on glass and placing it in an oven at 80 °C for 12 h to evaporate the solvents.

### 2.3. Fabrication of dye-sensitized $TiO_2$ photoanode

Nanocrystalline $TiO_2$ film was fabricated by a doctor-blading technique. The $TiO_2$ (P25) paste was deposited on a conducting glass substrate (F-doped $SnO_2$, 15 Ω $sq^{-1}$), followed by sintering at 500 °C for 30 min. The thickness of the film was 10 μm. The $TiO_2$ film was preheated at 120 °C for 30 min before it was immersed into the solution of the dye N3 ($Ru(dcbpy)_2(NCS)_2$, Solaronix) with a concentration of 0.5 mM in dry ethanol overnight.

### 2.4. Assembly of the dye-sensitized solar cell

The electrolyte solution was dripped onto the dyed $TiO_2$ film. Then the electrolyte was heated under 80 °C in oven until forming very viscous gel. Finally, a sandwich-type DSSC configuration was fabricated by holding the platinum plate counter electrode together with the $TiO_2$/electrolyte with two clips. All the cells based on PEO–PVDF polymer electrolytes were assembled and sealed in the oven at 80 °C to avoid the humidity. The measurements were performed in air. It should be noted that no 4-*tert*butylpyridine was added into the electrolyte.

### 2.5. Experimental measurements

#### 2.5.1. Differential scanning calorimetry (DSC) and IR study

Netzsch DSC 200PC (Germany) was used to measure the glass transition temperature ($T_g$) and melting temperature ($T_m$) of the polymer electrolyte membranes at a heating rate of 5 °C $min^{-1}$ from −100 to 200 °C under $N_2$ environment. FTIR measurements of the thin polymer electrolyte membranes were performed on a NEXUS670 (Nicolet) FTIR spectrometer from 4000 to 400 $cm^{-1}$, using the transmission mode.

#### 2.5.2. Rheology measurement

The viscosity of the PEO–PVDF polymer-blend electrolyte solutions with and without additives was measured by ARES (TA Instruments, USA), using the steady rate mode at 293 K. The apparent shear rate was varied from 10 to 800 $s^{-1}$.

#### 2.5.3. UV–vis spectra study

$I_3^-$ and $I^-$ absorption was performed in a U-shaped quartz tube with a quartz frit to support the sample by a UV-Vis-NIR Spectrophotometer (Cary 5000, Varian). The polymer-blend electrolyte solutions were dissolved in PC/DME co-solvent for this measurement.

#### 2.5.4. Impedance spectroscopy measurement

The ionic conductivity of the PEO–PVDF polymer-blend electrolyte films with and without additive were determined with an alternating current (AC) impedance technique on an AC impedance analyzer (Agilent 4294A, USA) from 40 Hz to 1 MHz between 20 and 80 °C (293 and 353 K) with signal amplitude of 10 mV. The polymer electrolyte was melted before a "platinum/electrolyte/platinum" type cell was assembled. The thickness of the polymer electrolyte membranes is controlled at 50 μm. The ionic conductivity $\sigma$ of the

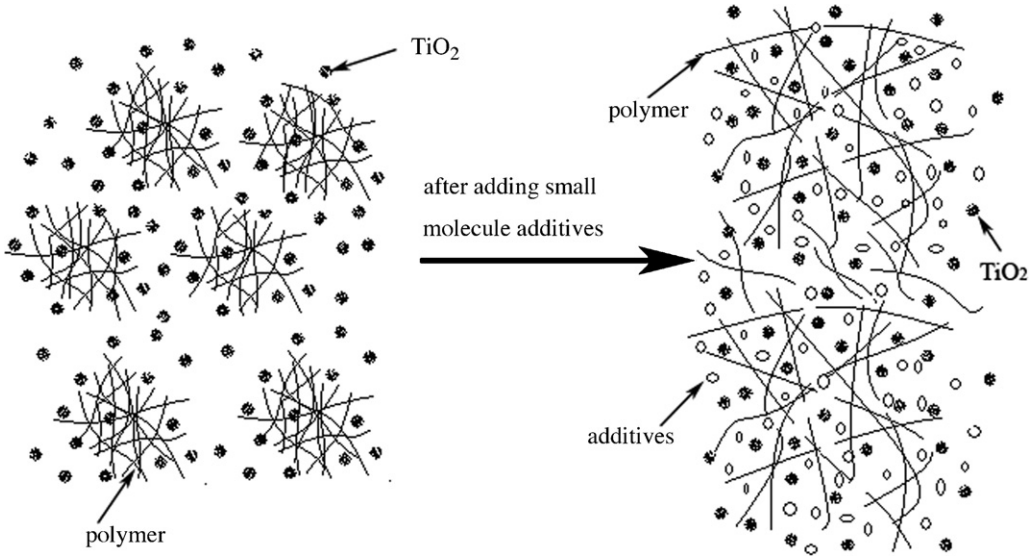


**Scheme 1.**

membrane is calculated by the following equation:

$$\sigma = \frac{L}{AR_b} \quad (1)$$

Here $L$ is the thickness of the polymer electrolyte membrane and $A$ is the area of the electrode. The resistance ($R_b$) is taken at the intercept of the Nyquist plot with the real axis. The temperature dependent conductivity of the polymer membrane was measured in a bench-top-type temperature and humidity chamber (Espec, Japan).

*2.5.5. SEM study*

The surface morphologies of the PEO–PVDF polymer-blend electrolyte films with and without additives were observed by scanning electron microscope (Sirion FEG, USA).

*2.5.6. Photoenergy conversion characterization*

Photon-to-current conversion efficiencies of the DSSC were evaluated by using a solar light simulator (Oriel, 91192) as the light source and a computer-controlled Keithley 2400 digital source meter unit (USA) as a current–voltage curve recorder. The intensity of the incident light was calibrated by a Si-1787 photodiode (spectral response range: 320–730 nm). The active DSSC area was controlled at 0.25 $cm^2$ by a mask. All of the measurements mentioned above were taken at ambient environment. Paraffin wax was used to temporarily seal the solar cells for quickly comparing the advantage of different electrolytes. After each measurement they were kept at room temperature.

## 3. Results and discussion

It is known, high-molecule-weight polymer (PEO with $M_w = 2 \times 10^6$ here) is tend to form aggregates by interwound interaction by itself, which increases the coil size of the polymer and results in ineffective electron transfer from polymer electrolyte to the dye molecules [22]. Water and ethanol are good small-molecule solvents to solvating PEO, which can act as a dispersant to interrupt the self-aggregate of polymer matrix and get more homogeneous solution. This is expected to be advantageous to salt dissociation and ionic conductivity. To understand the roles of these small-molecule additives playing in the PEO–PVDF/$TiO_2$ electrolyte, we propose a mode as shown in Scheme 1.

*3.1. FTIR analysis of PEO–PVDF polymer-blend electrolytes with and without additives*

FTIR analysis was employed to investigate the interaction between the polymer matrix and ethanol. Fig. 1 shows the FTIR spectra for PEO–PVDF polymer electrolyte with and without ethanol. Since PEO with a relatively high average molecular weight ($M_w = 2 \times 10^6$ g $mol^{-1}$) was used, the –OH absorption bands contributed by PEO should be negligible in the FTIR spectrum. The –OH absorption bands around 3400 $cm^{-1}$ due to the stretching vibration of –OH groups are attributed mainly to the surface hydroxyl in nano-$TiO_2$ particles. The –OH absorption peak shifts from 3436 $cm^{-1}$ to higher frequencies of 3439 $cm^{-1}$ and the C–O–C stretching peak in PEO shifts from 1097 to 1085 $cm^{-1}$ of the 3.1 wt.% ethanol-modified polymer electrolyte compared to that of unmodified one. This indicates the chemical cross-linking of –OH in $TiO_2$ with ethanol [23] and the hydrogen bonding formation between the C–O–C groups in PEO and the –OH groups of ethanol [24].

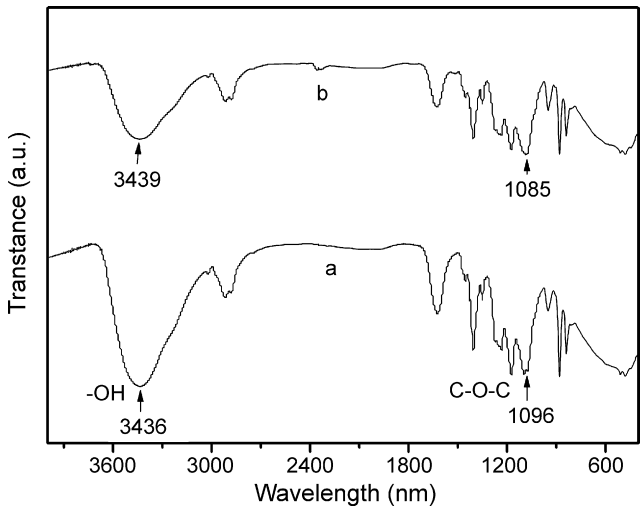


**Fig. 1.** FTIR spectra for: (a) poly (ethylene oxide)–poly (vinylidene fluoride) (PEO–PVDF) polymer electrolyte without additives; (b) 3.1 wt.% ethanol.

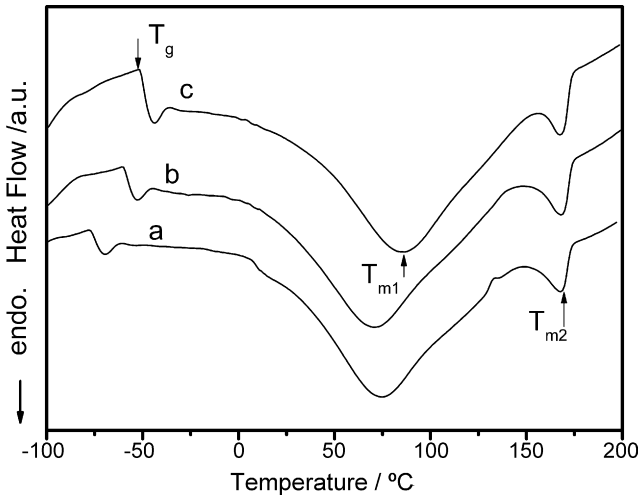


**Fig. 2.** DSC thermograms for: (a) poly (ethylene oxide)–poly (vinylidene fluoride) (PEO–PVDF) polymer electrolyte without additives; (b) 3.1 wt.% water; (c) 3.1 wt.% ethanol.

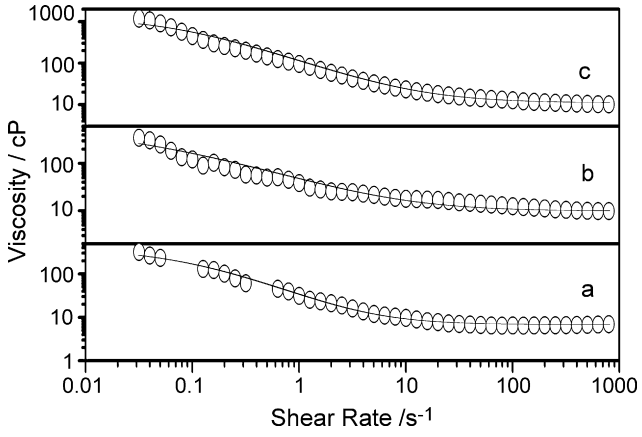


**Fig. 3.** The apparent viscosity change of the poly (ethylene oxide)–poly (vinylidene fluoride) (PEO–PVDF) polymer-blend electrolytes with different additives: (a) PEO–PVDF polymer electrolyte without additives; (b) 3.1 wt.% water; and (c) 3.1 wt.% ethanol. The apparent viscosity is recorded at an apparent shear rate from 10 to 800 $s^{-1}$ at temperature of 293 K. The solid lines are the fits of the Carreau–Yasuda model with parameters of the fit given in Table 1.

### 3.2. DSC characteristics of PEO–PVDF polymer-blend electrolytes with and without additives

Differential scanning calorimetry thermograms of pure PEO–PVDF polymer-blend electrolyte and the polymer-blend electrolytes with additives of water and ethanol are shown in Fig. 2 in the range between −100 and 200 °C. From the DSC thermograms, the glass transition temperature ($T_g$), the melting temperatures of PEO ($T_{m1}$), and PVDF ($T_{m2}$) were determined. Here, $T_m$ was obtained as the peak of the melting endotherm, and $T_g$ as the inflection point.

As shown in Fig. 2, the melting points around 48.4 and 168 °C of the PEO–PVDF polymer-blend electrolytes (Fig. 2a) are attributed to PEO and PVDF, respectively. All the electrolytes (Fig. 2a–c) show a single glass transition ($T_g$), which suggests that all the compositions are miscible with homogeneous phase in the polymer-blend electrolytes. When adding water and ethanol, the $T_g$ of the additive-modified electrolytes increase from −77.9 °C (un-added, Fig. 2a) to −60.5 °C (water added, Fig. 2b) and −51.8 °C (ethanol-added, Fig. 2c) as seen in Table 1, indicating a certain reduction of chain mobility by introducing these hydroxyl-rich additives. The increase in $T_g$ is probably due to the increased intercrossing bond formation among additives and the components in polymer electrolytes. The much more increase in $T_g$ of ethanol-added electrolyte compared to that of the water-added is may due to the stronger cross-linking ability of the –OH groups in ethanol than water with the EO units of PEO and –OH groups of $TiO_2$ in polymer matrix [25,26]. And the complexation effect of –OH in ethanol with the $Li^+$, which may also yields an increase in $T_g$ of electrolytes [27,28].

### 3.3. Rheological characteristics of PEO–PVDF polymer-blend electrolytes with different additives

The viscosity of the PEO–PVDF polymer-blend electrolyte solutions with and without additives was measured with apparent shear rate varied from 10 to 800 $s^{-1}$ at 293 K. All the electrolytes show a shear-thinning viscosity behavior. The measured shear viscosity for the polymer-blend electrolytes are fitted with the Carreau–Yasuda model, which is [29]:

$$\frac{\eta - \eta_\infty}{\eta_0 - \eta_\infty} = [1 + (\lambda\dot{\gamma})^a]^{(n-1)/a} \quad (2)$$

where $\eta_\infty$ is the infinite-shear viscosity, $\lambda$ is a time constant, and $1/\lambda$ is the critical shear rate at which viscosity begin to decrease, $(n-1)$ is the power-law exponent, and $a$ is a dimensionless parameter that describes the width of transition between the zero-shear region and the power-law region. We have chosen this model because it is quite flexible in fitting the non-Newtonian behavior of $\eta(\dot{\gamma})$ over a wide range of shear rates.

Changes of apparent viscosity with shear rates of different additive-modified electrolytes along with fits of the Carreau–Yasuda model as Eq. (2) (solid line) are presented in Fig. 3. The zero-shear viscosity ($\eta_0$), the final viscosity ($\eta_\infty$), and the parameters of Carreau–Yasuda equation $\lambda$, $a$ as well as $n$ are listed in Table 1.

As shown in Table 1, the zero-shear viscosities ($\eta_0$) of additive-modified electrolytes (water: 347.92 cP; and ethanol: 1175.9 cP) are higher than that of un-added one (319.16 cP), indicating a structural change in the PEO–PVDF polymer-blend electrolyte when introducing water and ethanol. The viscosity of polymer-blend electrolyte with different additives increases as: ethanol > water > un-added, which is consistent with the increasing trend of $T_g$ in DSC studies. With the increase of viscosity up to 1175.9 cP of ethanol adding electrolyte, the glass transition shifts to a higher temperature at −51.8 °C. We assume this change related to the increased intercrossing bond formation among the –OH groups of ethanol with the EO units of PEO, and –OH groups of $TiO_2$ in the polymer electrolytes as studied in Fig. 1, which reduces the chain mobility accompanied with an increase in viscosity.

**Table 1**
Thermal properties and Carreau–Yasuda model parameters for poly (ethylene oxide)–poly (vinylidene fluoride) (PEO–PVDF) polymer-blend electrolytes with different additives.

| Sample | $T_g$ (°C) | $\eta_0$ (cP) | $\eta_\infty$ (cP) | $\lambda$ (s) | $a$ | $n$ |
|---|---|---|---|---|---|---|
| PEO–PVDF polymer electrolyte | −77.9 | 319.16 | 6.96 | 11.96 | 0.948 | 0.048 |
| 3.1 wt.% water | −60.5 | 347.92 | 9.83 | 16.62 | 0.9777 | 0.2 |
| 3.1 wt.% ethanol | −51.8 | 1175.9 | 10.1 | 13.79 | 0.994 | 0.1 |

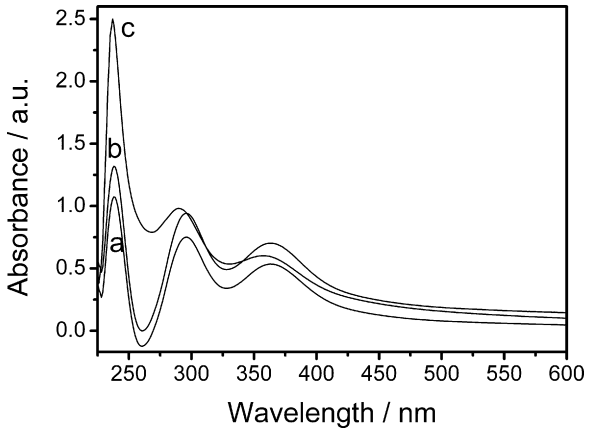


**Fig. 4.** UV–vis spectra of poly (ethylene oxide)–poly (vinylidene fluoride) (PEO–PVDF) polymer-blend electrolytes with and without additives: (a) PEO–PVDF polymer electrolyte without additives; (b) 3.1 wt.% water; and (c) 3.1 wt.% ethanol.

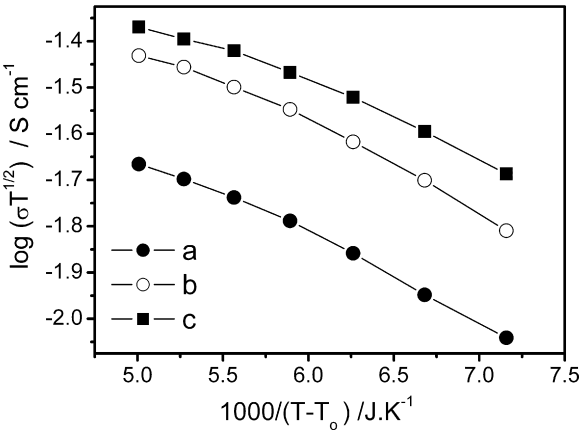


**Fig. 5.** Temperature dependence of ionic conductivity of poly (ethylene oxide)–poly (vinylidene fluoride) (PEO–PVDF) polymer-blend electrolytes with different additives: (a) PEO–PVDF polymer electrolyte without additives; (b) 3.1 wt.% water and (c) 3.1 wt.% ethanol.

The difference in viscosity behavior of water and ethanol-added electrolyte can be interpreted in the following manner. In the case of water-modified electrolyte, water behaves as a better solvent for the PEO than ethanol and exhibits weak interaction with PVDF [30]. In contrast to water, ethanol seems to act as stronger crosslinker between PEO and PVDF, which results in a larger viscosity of ethanol-added electrolytes than that of water-added electrolytes.

### 3.4. UV–vis study of PEO–PVDF polymer-blend electrolytes with different additives

The UV–vis absorptions of PEO–PVDF polymer-blend electrolytes with and without additives are shown in Fig. 4. As demonstrated, the peaks around 290 and 360 nm indicate the presence of $I_3^-$ [31] and around 226 nm is the peak of $I^-$ [32]. The intensity and width of the absorption peaks at 226 and 290 nm in the spectrum increase by introducing the additives, implying an increase in both $I^-$ and $I_3^-$ concentration in the electrolytes. Meanwhile, the peak intensity of $I^-$ at 226 nm of ethanol-added electrolyte is much enhanced compared to that of un-added one while there is no such obvious change in intensity of this peak when adding water. In the case of ethanol introducing, because the cross-linking effects among ethanol, $TiO_2$ and polymers are stronger than that in water-added electrolyte as mentioned above, the ethanol are expected to be retained in the electrolytes to provide sufficient –OH group to complex with $Li^+$ ions. This results in more movable $I^-$ ions in the electrolytes and an enhanced intensity of $I^-$ peaks as seen in Fig. 4a.

### 3.5. Conductivity of the PEO–PVDF polymer-blend electrolyte with and without additives

Fig. 5 illustrates the dependence of the conductivity of the PEO–PVDF polymer-blend electrolytes with different additives on temperature, which exhibits a typical Vogel–Tammann–Fulcher (VTF) conduction behavior, obeying the equation [33]:

$$\sigma(T) = AT^{1/2} \exp\left[\frac{-B}{\kappa(T - T_0)}\right] \quad (3)$$

where $\sigma$ and $T$ are the conductivity and absolute temperature respectively, $\kappa$ is the Boltzmann constant, $A$ is proportional to the number of the charge carriers, $T_0$ is regarded as 30–50 K below the measured $T_g$ [34] and $B$ is the activation energy. Here, $T_0$ is defined as $T_0 = T_g - 50$ (K), and $T_g$ as the glass transition temperature of the pure PEO–PVDF polymer blend [35].

The conductivity of PEO–PVDF polymer-blend electrolyte without additive at 30 °C is about $6.47 \times 10^{-4}$ S cm$^{-1}$ (Table 2), with an addition of water and ethanol, an increase in conductivity occurs compared to that of un-added one. The conductivity of polymer-blend electrolyte with different additives increases as: ethanol > water > un-added. The maximum value of $1.46 \times 10^{-3}$ S cm$^{-1}$ is achieved in the 3.1 wt.% ethanol-modified electrolyte.

As mentioned above, the viscosity and the glass transition temperature ($T_g$) of these PEO–PVDF polymer-blend electrolytes increase when the additives introduced. In general, the increase in viscosity lowers mobility of ions and hence conductivity should decrease. However, the increase in conductivity of these additive-modified electrolytes is observed, which may be due to the formation of continuous network through cross-linking between additives, PEO, $TiO_2$ and $Li^+$, expecting to be advantageous to ion transport in the electrolytes.

That is, the formation of efficient ion transport channels contributes to the increase of ionic conductivity. It plays more dominant role than that of the increased viscosity playing in the electrolytes [27,36]. However, care must be taken to differentiate of conductivity between water and ethanol. From UV–vis studies (Fig. 4), $I^-$ concentration of the electrolytes increases as: ethanol > water > un-added. In our previous studies [37], the ionic conductivity of PEO–PVDF polymer-blend electrolytes is dominated by anions ($I^-$) transport, and the increase in $I^-$ concentration

**Table 2**
Comparison of the parameters for cells based on poly (ethylene oxide)–poly (vinylidene fluoride) (PEO–PVDF) polymer-blend electrolytes with and without additive (the best one during stability test, 93.2 mW cm$^{-2}$, 0.25 cm$^{-2}$).

| Sample | $\sigma$ ($\times 10^{-3}$ S cm$^{-1}$) | $V_\infty$ | $J_{sc}$ (mA) | FF | $\eta$ (%) |
|---|---|---|---|---|---|
| PEO–PVDF polymer electrolyte | 0.647 | 560 | 8.92 | 0.491 | 2.63 |
| 3.1 wt.% water | 1.14 | 546 | 13.0 | 0.423 | 3.22 |
| 3.1 wt.% ethanol | 1.46 | 569 | 12.3 | 0.519 | 3.90 |

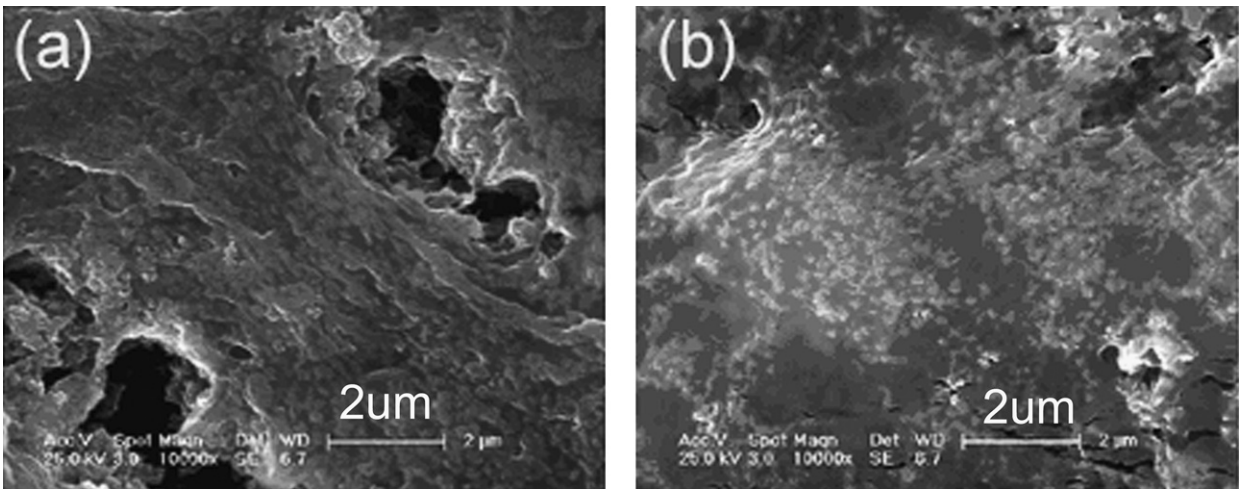


**Fig. 6.** SEM images of the poly (ethylene oxide)–poly (vinylidene fluoride) (PEO–PVDF) polymer-blend electrolytes based on: (a) without additives; (b) 3.1 wt.% ethanol-added.

in the electrolytes is expected helpful to the ionic conductivity of these additive-modified electrolytes. On the other hand, water is a better solvent to solvating the PEO compared to ethanol, which can play as a dispersant to prevent self-aggregates of the polymer matrix as seen in Scheme 1 to get more homogenous polymer solution. But ethanol are more subjected to form continuous network by its cross-linking terminal –OH groups with PEO and the surface –OH groups of nano-$TiO_2$ to provide more free $I^-$ ions in the electrolyte than water (Fig. 4) [25]. So we assume that, the higher conductivity of ethanol than water-modified electrolyte is attributed to the more contribution of the cross-linking ability of ethanol than that of water.

### 3.6. Additive effect on the surface morphology of PEO–PVDF polymer-blend electrolytes

Fig. 6 shows scanning electron microscopy of un-added and ethanol-added PEO–PVDF polymer-blend electrolyte membranes. A comparison of the surface morphology shows a marked change in the surface properties of the polymer-blend electrolyte thin films on addition of ethanol. Surface roughening, crystalline texture and agglomeration of internal morphology appear to change when adding the ethanol. The un-added PEO–PVDF polymer-blend electrolyte (Fig. 6a) displays a surface with rough texture and pores owing to the crystallization of the polymer matrix. However, as the 3.1 wt.% ethanol-added (Fig. 6b), the surface of texture becomes smooth and some amorphous regions are observed, showing a reduction of the crystallization. It is reasonable to assume that ethanol adding improves the compatibility between the inorganic particles and the polymer matrix so that miscibility between the materials is increased. And the use of small amount of ethanol as cross-linking agent contributes to improving the isolation of aggregated polymers which resulting in more homogeneous distribution of the polymer and $TiO_2$ and also enhances the opportunity for a continuous network through cross-linking with an expected increase in conductivity and stability.

### 3.7. Comparison of DSSC with the PEO–PVDF polymer-blend electrolyte and additive-modified PEO–PVDF polymer-blend electrolyte

Photocurrent density/voltage characteristics of N3-sensitized nanocrystalline $TiO_2$ film solar cells using PEO–PVDF polymer-blend electrolytes with various additives (water and ethanol) were measured under an illumination intensity of 93.2 mW cm$^{-2}$ (AM 1.5), and the results are presented in Fig. 7. Table 2 summarizes the results obtained from the *I–V* curves for DSSC assembled with different polymer electrolytes. A significant increase in performance is observed for the DSSC assembled with the water and ethanol-added polymer electrolytes. It shows that the $J_{sc}$ increases from 8.92 (un-added electrolyte) to 13 and 12.3 mA cm$^{-2}$ when adding 3.1 wt.% of water and ethanol, respectively. The best efficiency ($\eta$) of 3.9% is achieved in the cell with ethanol-adding electrolyte. These results imply that the additives (water and ethanol) are crucial in order to increase $J_{sc}$.

It is known that an efficient transport of iodide and triiodide in the electrolyte is necessary for good performance of the DSSC:

$$I^- + I_2 \leftrightarrow I_3^- + I_2 \leftrightarrow I_5^- \quad (4)$$

$$3I^- + 2dye^+ \rightarrow I_3^- + 2dye(TiO_2 photoanode) \quad (5)$$

$$I_3^- + 2e^- \leftrightarrow 3I^-(counterelectrode) \quad (6)$$

From the UV–vis study (Fig. 4), the introducing of water and ethanol increases the concentration of $I^-$ and $I_3^-$ in the additive-modified electrolytes. Since the ionic conductivity of PEO–PVDF electrolyte is dominated by anions ($I^-$) transport as we studied

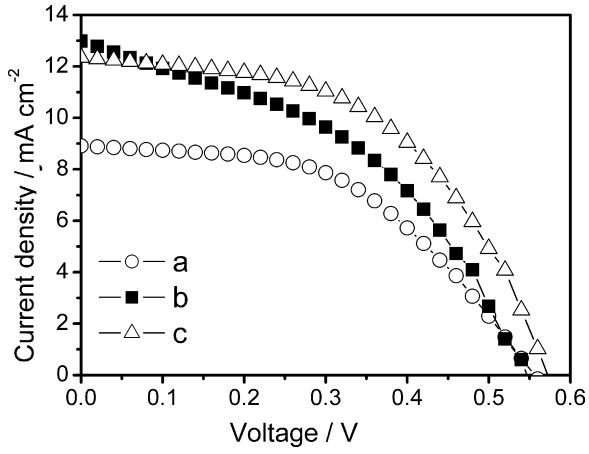


**Fig. 7.** Photocurrent–voltage curve of the DSSC with poly (ethylene oxide)–poly (vinylidene fluoride) (PEO–PVDF) polymer-blend electrolytes with and without additive (under AM 1.5 illumination 93.2 mW cm$^{-2}$, and cell active area 0.25 cm$^{-2}$): (a) PEO–PVDF polymer electrolyte without additive; (b) 3.1 wt.% water; and (c) 3.1 wt.% ethanol.

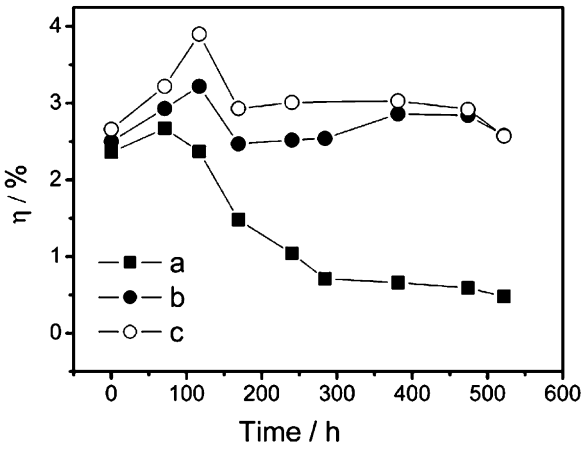


**Fig. 8.** Aging effect change of the photoconversion efficiency of the cells based on poly (ethylene oxide)–poly (vinylidene fluoride) (PEO–PVDF) polymer-blend electrolyte with and without additives: (a) PEO–PVDF polymer electrolyte without additives; (b) 3.1 wt.% water; and (c) 3.1 wt.% ethanol.

before [37]. The increase in $J_{sc}$ is associated with the increase in $I^-$ and $I_3^-$ concentration and the enhancement in ionic conductivity (Table 2), which provide more efficient $I^-/I^{3-}$ transportation in the additive-modified electrolytes due to the increased free ion ($I^-/I^{3-}$) concentration and ion transport network channels between additives, salt and polymer matrix.

### *3.8. Stability of DSSC based on PEO–PVDF polymer-blend electrolyte with and without additives*

The evolution of photo-to-current efficiency ($\eta$) with time for cells based on PEO–PVDF polymer-blend electrolyte with and without additives is presented in Fig. 8. The improved long-term stability of the cells based on additive-modified electrolytes is observed compared to that of un-added one. The performance of the cell based on un-added electrolyte shows a decrease of 80% in efficiency after 522 h. And the cell performances based on water and ethanol-added electrolytes remain constant for almost 522 h. Since wax was used here to seal the cell devices for quick comparing, a higher stability should be obtained after sealing optimization.

Our stability tests corroborate the data obtained from DSC and SEM analysis, the improved stability of cell efficiency based on the additive-modified electrolytes can be related to the cross-linking network between additives (water and ethanol), salt and polymer matrix, which remains these small-molecule solvents in polymer host to contribute to the ionic conductivity and the long-term stability of the efficiency. As for the cell of un-added electrolyte, since it did not form the continuous network as efficient as the additive-modified ones, there are empty spaces as seen in SEM study (Fig. 6) which lead to increased resistance and lowered contact with the electrode, and damage the stability of DSSC.

## 4. Conclusions

The addition of water and ethanol to PEO–PVDF polymer-blend electrolyte having conductivity higher than that of un-added one, resulted in more homogenous gel polymer electrolyte with conductivity of the order of $10^{-3}$ S cm$^{-1}$ along with higher viscosity. The increased ionic conductivity was assumed to be due to an increase in free ion concentration and enhanced cross-linking network channels by adding additives. The addition of water and ethanol improved the photovoltaic performances and long-term stability of the corresponding DSSC. The best efficiency of 3.9% was achieved in the cell based on ethanol-modified electrolyte. The stability of the cells based on water and ethanol-added electrolytes had been found to be stable up to almost 522 h.

## Acknowledgments

We acknowledge the financial support of the Ministry of Science and Technology of China through Hi-Tech plan (funding no. 2006AA03Z347) and partial financial support from the National Nature Science Foundation of China (50125309). We also acknowledge the help of the Nanoscience and Nanotechnology Centre at Wuhan University for the DSC and SEM measurements.

## References

[1] B. O'Regan, M. Grätzel, Nature 353 (1991) 737.
[2] M. Grätzel, Inorg. Chem. 44 (2005) 6841.
[3] Q.B. Meng, K. Takahashi, X.T. Zhang, I. Sutanto, T.N. Rao, O. Sato, A. Fujishima, Langmuir 19 (2003) 3572.
[4] N. Hirata, J.E. Kroeze, T. Park, D. Jones, S.A. Haque, A.B. Holmes, J.R. Durrant, Chem. Commun. (2006) 535.
[5] P. Wang, S.M. Zakeeruddin, J.E. Moser, M. Gra1tzel, J. Phys. Chem. B 107 (2003) 13280.
[6] W. Kubo, S. Kambe, S. Nakade, T. Kitamura, K. Hanabusa, Y. Wada, S. Yanagida, J. Phys. Chem. B 107 (2003) 4374.
[7] H. Yang, C.Z. Yu, Q.L. Song, Y.Y. Xia, F.Y. Li, Z.G. Chen, X.H. Li, T. Yi, C.H. Huang, Chem. Mater. 18 (2006) 5173.
[8] L. Wang, S. Fang, Y. Lin, X. Zhou, M. Li, Chem. Commun. (2005) 5687.
[9] P. Wang, S.M. Zakeeruddin, J.E. Moser, M.K. Nazeeruddin, T. Sekiguchi, M. Gratzel, Nat. Mater. 2 (2003) 402.
[10] T. Stergiopoulos, I.M. Arabatzis, G. Katsaros, P. Falaras, Nano Lett. 2 (2002) 1259.
[11] J.H. Kim, M.S. Kang, Y.J. Kim, J. Won, N.G. Park, Y.S. K, Chem. Commun. (2004) 1662.
[12] J.B. Xia, F.Y. Li, C.H. Huang, J. Zhai, L. Jiang, Sol. Energy Mater. Sol. Cells 90 (2006) 944.
[13] W. Kubo, T. Kitamura, K. Hanabusa, Y. Wada, S. Yanagida, Chem. Comm. (2002) 374.
[14] W. Kubo, K. Murakoshi, T. Kitamura, S. Yoshida, M. Haruki, K. Hanabusa, H. Shirai, Y. Wada, S. Yanagida, J. Phys. Chem. B 105 (2001) 12809.
[15] S. Murai, S. Mikoshiba, H. Sumino, S. Hayase, J. Photochem. Photobiol. 148 (2002) 33.
[16] J. Kang, W. Li, X. Wang, Y. Lin, X. Xiao, S. Fang, Electrochim. Acta 48 (2003) 2487.
[17] D.K. Pradhan, B.K. Samantaray, R.N.P. Choudhary, A.K. Thakur, J. Power Sources 139 (2005) 384.
[18] K. Edelmann, B. Sandner, Solid State Ionics 170 (2004) 225.
[19] M.M.E. Jacob, S.R.S. Prabaharan, S. Radhakrishna, Solid State Ionics 104 (1997) 267.
[20] H.W. Han, W. Liu, J. Zhang, X.Z. Zhao, Adv. Funct. Mater. 15 (2005) 1940.
[21] J. Zhang, H.W. Han, S.J. Wu, S. Xu, C.H. Zhou, Y. Yang, X.Z. Zhao, Nanotechnology 18 (2007) 295606.
[22] Y.J. Kim, J.H. Kim, M.S. Kang, M.J. Lee, J. Won, J.C. Lee, Y.S. Kang, Adv. Mater. 16 (2004) 1753.
[23] M.S. Kang, J.H. Kim, J. Won, Y.S. Kang, J. Photochem. Photobiol. A 183 (2006) 15.
[24] X. Zhu, Y. Xiao, P. He, D. Yan, Y. Fang, Polym. Int. 52 (2003) 813.
[25] M.S. Kang, J.H. Kim, J. Won, Y.S. Kang, J. Photoch. Photobiol. A: Chem. 183 (2006) 15.
[26] K. Mimura, H. Ito, H. Fujioka, Polymer 41 (2000) 4451.
[27] K.H. Lee, Y.G. Lee, J.K. Parka, D.Y. Seung, Solid State Ionics 133 (2000) 257.
[28] H. Masui, M.E. Williams, J.W. Long, M. Troutman, R.W. Murray, Solid State Ionics 107 (1998) 175.
[29] Y. Heo, J. Rheol. 49 (2005) 1117.
[30] D.L. Wang, K. Li, W.K. Teo, J. Membr. Sci. 178 (2000) 13.
[31] Z. Kebede, S.E. Lindquist, Sol. Energy Mater. Sol. Cells 57 (1999) 259.
[32] C.B. Allsopp, Proc. R. Soc. Lond. Ser. A: Math. Phys. Sci. (January) (1937) 167.
[33] J.S. Gnanaraj, R.N. Karekar, S. Skaria, C.R. Rajan, S. Ponrathnam, Polymer 38 (1997) 3709.
[34] M. Siekierski, W. Wieczorek, J. Przyłuski, Electrochim. Acta 43 (1998) 1339.
[35] F. Croce, R. Curini, S. Pantaloni, A. Selvaggi, B. Scrosati, J. Appl. Electrochem. 18 (1998) 401.
[36] J.P. Sharma, S.S. Sekhon, Solid State Ionics 178 (2007) 439.
[37] Y. Yang, J. Zhang, C.H. Zhou, S.J. Wu, S. Xu, W. Liu, H.W. Han, B.L. Chen, X.-Z. Zhao, J. Phys. Chem. B 112 (2008) 6594.